WATER RESOURCES RESEARCH, VOL. 27, NO. 9, PAGES 2219–2232, SEPTEMBER 1991

A Comparison of Four Inverse Approaches to Groundwater Flow and Transport Parameter Identification

ALLAN KEIDSER AND DAN ROSBJERG

Groundwater Research Centre, Technical University of Denmark, Lyngby

Four different methods of parameterizing spatially varying log transmissivities in an inverse approach are compared with respect to prediction accuracy of simulated flow and transport. Transport parameter estimation is included by two-stage feedback optimization. In stage one the log transmissivities are estimated by fitting both head and concentration data, given initial values of the source concentration and the dispersivities. In stage two, the source concentration and the dispersivities are estimated by fitting the concentration data. With the updated transport parameters, final estimates of the log transmissivities are obtained by repeating the optimization of stage one. The formulated objective functions are minimized using Levenberg-Marquardt's algorithm. The models are applied to synthetic two-dimensional transport problems in steady state flow regimes. The "true" log transmissivity fields are generated by the turning bands method, thereby incorporating spatial variability. The test cases differ in the input variances of the generated fields and with respect to the amount and accuracy of "observed" transmissivity data.

1. INTRODUCTION

1.1. *Background*

Numerical models are powerful tools when dealing with groundwater quality management. In recent years, the importance of such models has increased with the appearance of increasingly serious groundwater contamination problems in the industrialized parts of the world.

Numerical models require a number of parameters characterizing the aquifer. Usually, prior knowledge of the values of these parameters is limited, and they must be quantified by calibration which uses observations of hydraulic heads and solute concentrations. Most commonly the parameters are estimated by using a "trial and error" approach. Because the number and combinations of parameter adjustments are not bounded, "trial and error" is rather flexible but also time-consuming. Additionally, the solution is strongly dependent on the skill of the practitioner.

During recent years, inverse techniques in groundwater flow modeling have made their appearance. Inverse models identify unknown parameters (so-called model parameters) by using mathematical optimization techniques. The objective is to minimize a functional of the discrepancies between observed and calculated heads (and/or concentrations, when transport is included). Furthermore, if model parameter estimates are considered as random variables, then statistical estimation procedures become applicable, and the reliability of the simulation model can be assessed.

The inverse solutions are strongly influenced by instability and nonuniqueness (the inverse problem is said to be "ill-posed"). The difficulty of overcoming ill-posedness is the main reason why inverse techniques have not become standard tools in quantitative flow modeling. Instability often appears as large fluctuations and nonrealistic estimates of distributed parameters. Nonuniqueness is due to nonidentifiability of one or more model parameters or to the occurrence of several local minima of the objective function. One phenomenon is often mistaken for another, e.g., instability caused by a poorly defined minimum is often mistaken for nonuniqueness as both lead to different solutions dependent on the starting point of the iterative algorithm.

There are relatively few examples of inverse models in the literature involving solute transport. This is partly due to the lack of well-studied transport cases. Furthermore, the problems of ill-posedness characterizing inverse flow modeling are inevitably still more pronounced when the estimation procedure is further complicated by adding transport. Reviews of methods and concepts related to the inverse problem are presented by, e.g., *Yeh* [1986] and *Carrera* [1987].

Concerning the forward modeling, solute transport is a complex phenomenon, and it is difficult even to identify the relevant transport processes. *Knopman and Voss* [1988] make a coupled optimization of model identification and parameter estimation. They discriminate between alternative, predescribed transport models involving different transport processes. In the following, the governing transport processes are assumed to be known, and only parameter estimation is considered.

1.2. *Previous Work*

Inverse transport modeling is difficult when flow and transport parameters are optimized simultaneously because of slow convergence rates and unstable estimates. As a result, the flow parameters have often been assumed to be known. *Murphy and Scott* [1977] introduced an inverse approach in order to estimate the dispersivities from observed concentration values. For each set of observations they developed concentration polynomials by using double interpolation. If the estimation is based on just two observed values, the solution is unique. In the case of more than two observations, the two model parameters were estimated iteratively by nonlinear least squares regression. *Umari et al.* [1979] estimated the dispersivities too, by minimizing discrepancies between observed and calculated concentration values. They used a finite element discretization of the transport equation to calculate concentrations. *Gorelick et al.* [1983] used the location and magnitude of the pollutant

Paper number 91WR00990.
0043-1397/91/91WR-00990$05.00

sources as unknown model parameters. They tested different minimization criteria involving predicted concentration residuals. By normalizing the residuals with the observed values, more accurate estimates were obtained compared to models using ordinary residuals.

The approach of *Adar et al.* [1988] differs in using transport data to estimate flow parameters. The unknown values were rates of recharge into the aquifer, while knowledge of the transport parameters was implied. The recharge parameters were calculated by minimizing a weighted sum of squared mass balance errors including both water and conservative chemical species.

Strecker and Chu [1986] were the first to estimate both flow and transport parameters in an inverse approach. They reduced the difficulties of stability by dividing the optimization procedure into two separate stages. In stage one the transmissivity field was estimated, and in stage two the transport problem was treated with the dispersivities as model parameters. The optimization in stage one was based on head data only. Since the solute spreading also depends on the transmissivity, the method does not fully utilize the information inherent in the concentration data. *Wagner and Gorelick* [1987] estimated flow and transport parameters simultaneously by inverse modeling. The model parameters were the log conductivity, the effective porosity, and the dispersivities. They made use of nonlinear regression based on the least squares method, which allowed uncertainties of both optimized model parameters and simulated concentrations to be estimated.

Both *Strecker and Chu* [1986] and *Wagner and Gorelick* [1987] make use of simple, synthetic transport problems, and in both cases the reproduction of the solute spreading was based on the assumption of homogeneous transmissivity. *Van Rooy et al.* [1989] applied different inverse models of the two-stage type to a nonhomogeneous hypothetical aquifer. A spatially variable transmissivity field was generated by the turning bands method [*Mantoglou and Wilson*, 1982]; in stage one the model reproduced the transmissivity field by kriging, while the source concentration and the dispersivities were estimated in stage two. Different kriging input functions were tested, and the kriging estimates were based on different sets of transmissivity "observations." The modeling of the spatially variable transmissivity was shown to be important to simulate solute spreading accurately.

Keidser et al. [1990] extended the two-stage approach to a two-stage feedback procedure. The model parameters were divided into transmissivity values as flow parameters, and source concentration and dispersivities as transport parameters. By including concentration data in the transmissivity estimation, the transmissivity parameters and the transport parameters were optimized iteratively. The application of the procedure to a field problem resulted in a rapid convergence: No significant improvements occurred after the first run of the iteration loop.

1.3. *Scope of Present Contribution*

This study deals with inverse transport modeling, but the most attention will be paid to the transmissivity estimation, thereby utilizing the experience of *Van Rooy et al.* [1989].

The problem of stability characterizing inverse models in groundwater hydrology points toward multistage solution procedures. Therefore, the applied techniques are based on the two-stage approach. In the first stage the transmissivity field is estimated using both head and concentration data. Transferring the estimated transmissivity field to the second stage, the transport parameters are optimized on the basis of the concentration measurements. Finally, the stage one estimation is repeated to adjust the transmissivity parameters using the optimized transport parameters.

To reproduce the spatially variable transmissivities, four different approaches are formulated. For that purpose four different sets of transmissivity-related parameters are formulated as model parameters in stage one. Further, the models differ in the way prior information of transmissivity is used. Three of the models reproduce point observations of transmissivity in the estimated field by means of kriging. One approach supplies the observations with estimated transmissivity values, the second adjusts the kriging estimates by means of correcting terms, and the third adjusts the kriging model by optimizing the geostatistics of the transmissivity. In that way the three kriging approaches result in different constraints of the transmissivity field by the incorporated transmissivity information. Finally, in the fourth approach the observations are not used directly in the transmissivity estimation. The approach is based on zonation, and the inherent information is utilized to develop the zonation pattern.

The test cases are based on synthetic aquifers that are constructed to resemble real life fields in regard to complexity and erratic behavior.

The sensitivity of each model to the quantity and quality of the observed transmissivity data and the ability of the models to reproduce transmissivity fields of different complexity are analyzed.

To compare the different models, test measures of simulation accuracy are formulated. Furthermore, "future" predictions are carried out and compared with synthetic simulations. Thereby advantages and weaknesses of each model are identified, and guidelines for model choice in real life transport modeling are given.

2. METHODOLOGY

2.1. *Theory*

The present paper deals with two-dimensional steady state flow and nonsteady transport of nonreactive solutes in the saturated groundwater zone. The governing mathematical equations are [*Bear*, 1972]

$$\text{div}\ (\mathbf{T}\ \text{grad}\ h) - R = 0 \tag{1}$$

$$\text{div}\ (\mathbf{D}\ \text{grad}\ C) - \frac{\mathbf{q}\ \text{grad}\ C}{\theta} - \frac{C'R}{b\theta} = \frac{\partial C}{\partial t} \tag{2}$$

$\mathbf{T}$ transmissivity tensor $[L^2T^{-1}]$;
h hydraulic head $[L]$;
R volume flux per unit area of fluid sinks or sources (positive for outflow) $[LT^{-1}]$;
$\mathbf{q}$ Darcy velocity vector $[LT^{-1}]$;
b saturated thickness $[L]$;
$\mathbf{D}$ hydrodynamic dispersion tensor $[L^2T^{-1}]$;
C solute concentration $[ML^{-3}]$;
θ effective porosity:
C' solute concentration in sink or source fluid (for sinks $C' = C$)$[ML^{-3}]$.

TABLE 1. Transmissivity Modeling Characteristics of the Four Inverse Approaches

	F1	F2	F3	F4
Basic approach	kriging	kriging and zonation	kriging	zonation
Y observations incorporated	yes	yes	yes	no
Prior determination needed	geostatistics of Y and pilot point locations	geostatistics of Y and zonal pattern	...	zonal pattern
Model parameters	pilot point transmissivities	zonal correcting factors	trend parameters and correlation structure parameters	zonal transmissivities

estimated trend is artificially conditioned on the location of observation points. In fact, three of the approaches are different methods for compensating these disadvantages. The fourth approach is based on zonation, and kriging is only used in the initial stage of developing the zonal pattern as no specific geological information to support the zonation is assumed available. Apart from the Y field modeling the four approaches are kept identical, including the degree of freedom (the number of h/C observations minus the number of model parameters).

The first of the inverse models, which is designated F1, estimates the Y distribution by point kriging. The model parameters which are to be optimized are the Y values at selected aquifer points called "pilot points." The method was introduced by *de Marsily et al.* [1984], who fitted observed pressure records from interference tests by using least squares minimization. In this study there are seven pilot points, so that

$$\mathbf{p}_{f_1} = (Y_{p_1}, Y_{p_2}, \cdots, Y_{p_7}) \tag{10}$$

To produce the entire Y field, the optimized Y values are used jointly with the measured values as kriging "observations."

Method F1 requires that the correlation structure of the Y field is known. This can be estimated by a semivariogram analysis (in real life cases previous analysis of similar aquifers can be applied too). In this study the semivariogram is derived by using an automatic optimization procedure based on the maximum likelihood approach [*Samper and Neuman*, 1989]. By treating the cross-validation errors of kriged Y values as Gaussian, a likelihood function can be formulated based on the chosen semivariogram. Then the parameters quantifying the semivariogram are optimized by minimizing the negative log likelihood (NLL) of the errors. By assuming that the errors are uncorrelated, NLL is given by

$$\mathrm{NLL} = N \ln 2\pi + \sum_{i=1}^{N} \ln \sigma_i^2 + \sum_{i=1}^{N} \frac{e_i^2}{\sigma_i^2} \tag{11}$$

where σ_i^2 is the kriging variance of the ith cross-validation error e_i. Lacking other information, the semivariogram analysis is based on the assumption of stationarity. *Samper and Neuman* [1989] tested different model selection criteria, which depend on the number of Y observations and the number of parameters to be optimized. In the present study three semivariogram models have been tested. As both the number of unknown model parameters and the number of Y observations are identical, the minimum value of NLL itself has been used as the selection criterion.

The IMSL minimization algorithm DBCONF was used to minimize (11). The algorithm uses a quasi-Newton method with a finite difference approximation to the gradient vector [*IMSL*, 1987].

The second inverse model, F2, is a heuristic approach introduced by *Keidser et al.* [1990] to combine the flexibility of the zonation approach with the increased plausibility obtained by taking information about the Y field into account. Based on knowledge of the correlation structure obtained as in the application of the F1 model, nodal kriging estimates Y^*, and kriging variances σ_Y^{2*} are calculated. Then correcting terms proportional to σ_Y^* are added to the estimates. By dividing the aquifer into subregions, the final Y estimate is calculated as

$$\hat{Y} = Y^* + k\sigma_Y^* \tag{12}$$

where k is a region-specific correcting factor to be optimized. This allows Y to vary within each zone, whereas classical zoning assigns a single Y value to the entire zone. By dividing the aquifer into seven zones, the model parameters are the seven corresponding correcting factors

$$\mathbf{p}_{f_2} = (k_1, k_2, \cdots, k_7) \tag{13}$$

The third kriging approach, F3, optimizes the parameters of the geostatistical description of the Y field. The geostatistics are formulated by means of a trend function and an autocovariance function. The idea of estimating the parameters quantifying the kriging model was introduced by *Kitanidis and Vomvoris* [1983] to solve simple one-dimensional problems, and extended by *Hoeksema and Kitanidis* [1984] for two-dimensional application. They eliminated the estimation of trend parameters by assuming spatial stationarity. The model parameters were optimized as maximum likelihood estimates, based on the joint probability distribution of observed heads and log conductivities. *Kuiper* [1986] incorporated a linear trend and ordinary least squares minimization of predicted head residuals into the method. *Van Rooy et al.* [1989] used the least squares criterion to estimate the trend and correlation length of the Y field. The approach formed the first stage of a two-stage inverse transport procedure in which, among other things, a linear trend was compared to a second-order trend of the transmissivity field. The second-order model gave the closest fit of the concentration plume in the far-field region. In the present study the second-order model for the mean transmissivity is used, and is expressed as

Hydrodynamic dispersion is assumed to equal mechanical dispersion, and other processes are considered negligible. Assuming aquifer isotropy, the coefficients of the dispersion tensor can be defined as [*Bear*, 1972]

$$D_L = \beta_L|\mathbf{v}| \tag{3}$$

$$D_T = \beta_T|\mathbf{v}| \tag{4}$$

D_L, D_T longitudinal and transverse dispersion coefficients corresponding to the flow direction $[L^2T^{-1}]$;
β_L, β_T longitudinal and transverse dispersivities $[L]$;
$|\mathbf{v}|$ magnitude of the seepage (or pore water) velocity vector ($\mathbf{v} = \mathbf{q}/\theta$) $[LT^{-1}]$.

The dispersivities, β_L and β_T, are not constants, but depend on the time or length scale of the transport process [e.g., *Dagan*, 1982].

The hydraulic head, h, and the solute concentration, C, are the dependent variables of the governing equations, and their accuracy depends on knowledge of the physical parameters T, R, β_L, β_T, θ and C'. In the inverse approach, unknown or incompletely known physical parameters are selected as model parameters that are to be estimated using observed values of h and C.

2.2. *Parameter Identification Procedure*

The transmissivity, T, is considered to be stochastically distributed. That is, the parameter is randomly varying, and its statistical behavior is a function of spatial location. Log transmissivity $Y = \ln T$ is considered instead of T to avoid solutions with negative values of T. Further, as T is known from experience to be lognormally distributed [e.g., *Freeze*, 1975], working with Y lends some optimality properties to methods such as kriging.

The model parameters are divided into two groups: the flow parameters $\mathbf{p}_f$, which are used to define the Y field, and the transport parameters $\mathbf{p}_t = (\beta_L, \beta_T, C')$.

The hydraulic head, h, is assumed to be measured at M locations, and the concentration C at L locations of the aquifer. The solute stems from a point source, and the time and location of the leakage are assumed to be known.

Model parameters are estimated by a two-stage feedback procedure. In stage one, the parameters $\mathbf{p}_f$ are estimated by using the generalized least squares model fit criterion. The criterion fits the calculated to observed values of head and concentration by minimizing the objective function

$$J_f(\hat{\mathbf{p}}_f|\mathbf{p}_t) = J_h(\hat{\mathbf{p}}_f) + J_C(\hat{\mathbf{p}}_f|\mathbf{p}_t) \tag{5}$$

where

$$J_h(\hat{\mathbf{p}}_f) = [\hat{\mathbf{h}}(\hat{\mathbf{p}}_f) - \bar{\mathbf{h}}]^T \mathbf{W}_h [\hat{\mathbf{h}}(\hat{\mathbf{p}}_f) - \bar{\mathbf{h}}] \tag{6}$$

$$J_C(\hat{\mathbf{p}}_f|\mathbf{p}_t) = [\hat{\mathbf{C}}(\hat{\mathbf{p}}_f|\mathbf{p}_t) - \bar{\mathbf{C}}]^T \mathbf{W}_C [\hat{\mathbf{C}}(\hat{\mathbf{p}}_f|\mathbf{p}_t) - \bar{\mathbf{C}}] \tag{7}$$

Here characters with tildes and circumflexes designate observed and calculated values, respectively. $\mathbf{W}_h$ and $\mathbf{W}_C$ are weight matrices. The superscript T indicates the transpose. The calculation of $\hat{\mathbf{C}}$ is based on initial guesses of the transport parameters $\mathbf{p}_t$. In stage two, the estimated Y field is used, and $\mathbf{p}_t$ is optimized by minimizing the objective function

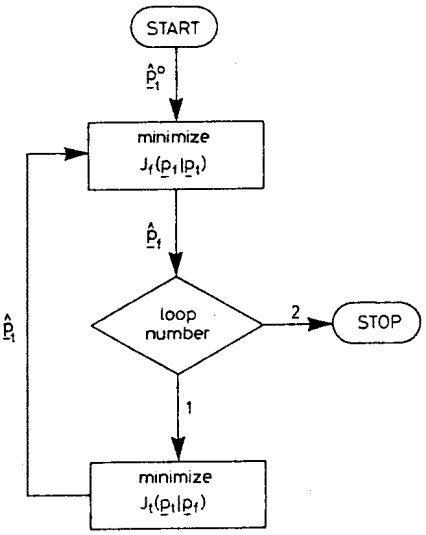

Fig. 1. Diagram of the superior feedback loop.

$$J_t(\hat{\mathbf{p}}_t|\mathbf{p}_f) = [\hat{\mathbf{C}}(\hat{\mathbf{p}}_t|\mathbf{p}_f) - \bar{\mathbf{C}}]^T \mathbf{W}_C [\hat{\mathbf{C}}(\hat{\mathbf{p}}_t|\mathbf{p}_f) - \bar{\mathbf{C}}] \tag{8}$$

Finally, stage one is repeated to adjust the transmissivity parameters, $\mathbf{p}_f$, using the optimized transport parameters. The optimization procedure is shown in Figure 1.

The models imply knowledge of the weight matrices $\mathbf{W}_h$ and $\mathbf{W}_C$. Assuming the correlation between measurement errors to be negligible, only diagonal elements of the matrices are nonzero. In the present study, $\mathbf{W}_h$ is set equal to the unit matrix, while the diagonal elements $w_{C_{ii}}$ of $\mathbf{W}_C$ are weighted with respect to the observed values of C:

$$w_{C_{ii}} = (\bar{C}_i + \eta)^{-2} \qquad i = 1, 2, \cdots, L \tag{9}$$

The expression is based on the fact that the differences $\hat{\mathbf{C}} - \bar{\mathbf{C}}$ tend to be proportional to the observed values at large concentrations, while tending to a constant at low concentrations. Thus, the constant η is added to prevent large relative differences at low concentrations to dominate [*Van Rooy et al.*, 1989].

The groundwater model selected for the study is the one developed at the U.S. Geological Survey by *Konikow and Bredehoeft* [1978]. The model makes use of the method of characteristics (MOC) approach to solve the solute transport equation.

The objective functions (5)–(7) and (8) are minimized using the IMSL version DBCLSF of the Levenberg-Marquardt algorithm. The routine uses a finite difference approximation to the Jacobian matrix [*IMSL*, 1987].

2.3. *Transmissivity Field Modeling*

To reproduce the log transmissivity field, four different models are formulated as briefly sketched in Table 1. Point observations of Y at N locations of the aquifer are assumed to be available.

All four approaches are more or less based on kriging, which is very suitable to inverse modeling as it estimates a random field from a few statistical parameters. The description of spatially distributed parameters by simple functional expressions is essential in order to avoid instability. On the other hand, kriging smooths out spatial variations, and the

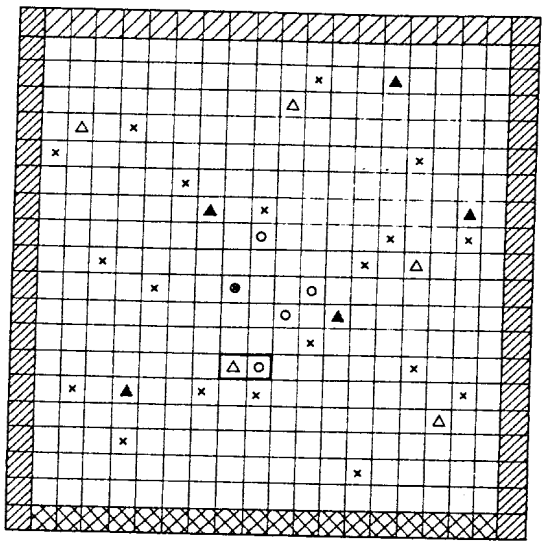

Fig. 2. The fictitious aquifer and locations of "observation" data (the nodal distance is 200 m).

transport data. In test case 4 the pilot points and zonations from test case 1 are retained. On the basis of test case 4, the models F1 and F2 are further tested with respect to their sensitivity to the formulated geostatistical model and to the prior determination of pilot point locations and zonation pattern, respectively.

All other parameters and conditions not described above are kept identical in the different test cases. By setting the constant η in (9) to 100 mg/L a reasonable weighting of the concentration residuals is obtained. The different conditions represented by the test cases concern the transmissivity only, and analysis of the sensitivity to noise in head and concentration data is beyond the scope of the paper.

3.2. *Measures of Prediction Accuracy*

Two types of prediction accuracy are considered. The first type accounts for the ability to fit the "observation" data. The two measures of "data fit" used are

$$\mathrm{HDF} = \frac{1}{M} \sum_{i=1}^{L} (\hat{h}_i - \bar{h}_i)^2 \tag{20}$$

$$\mathrm{CDF} = \frac{1}{L} \sum_{i=1}^{L} w_{c_{ii}} (\hat{C}_i - \bar{C}_i)^2 \tag{21}$$

The applied symbols are defined in section 2.2.

The second type accounts for the ability to fit the entire distribution of head and concentration. Two measures of "model fit" are formulated:

$$\mathrm{HMF} = \frac{1}{n} \sum_{i=1}^{n} (\hat{h}_i - h_i)^2 \tag{22}$$

$$\mathrm{CMF}_{18} = \left[\frac{1}{n_c} \sum_{i=1}^{n_c} w_i (\hat{C}_i - C_i)^2 | \text{transport period} = 18 \text{ years} \right] \tag{23}$$

In (22) and (23) n and n_c are the number of finite difference nodes and the number of nodes influenced by the C plume, respectively. The h_i and C_i are nodal values of the "real" synthesized distributions, and the w_i are calculated by means of (9) with C_i substituted for $\bar{C}_i$.

A further measure is formulated accounting for the ability of the models to fit a future situation (40 years transport period):

$$\mathrm{CMF}_{40} = \left[\frac{1}{n_c} \sum_{i=1}^{n_c} w_i (\hat{C}_i - C_i)^2 | \text{transport period} = 40 \text{ years} \right] \tag{24}$$

CMF_{40} acts as a measure of "prediction performance" to indicate the reliability of the estimated model parameters.

3.3. *Semivariogram Analysis*

For each of the two generated fields, 10 Y "observations" are selected. On the basis of this prior information the semivariograms to be used as input to the kriging approaches of F1 and F2 are estimated.

The incorporated trend is not taken into account as no

$$\bar{Y}(x, y) = \theta_1 + \theta_2 x + \theta_3 y + \theta_4 x^2 + \theta_5 y^2 + \theta_6 xy \quad (14)$$

The θ are the unknown coefficients quantifying the trend. The semivariogram analysis carried out in the application of F1 and F2 leads to a Gaussian model (section 3.3). For the sake of equality, the Gaussian expression also is used for the autocovariance in the F3 approach:

$$\mathrm{Cov}_Y(r) = \sigma_Y^2 \exp(-\alpha^2 r^2) \quad (15)$$

where r is the spatial lag, σ_Y^2 is the variance, and α is the reciprocal correlation length. The unknown parameters in (14)–(15) are

$$\mathbf{p}_{f_3} = (\alpha, \theta_1, \theta_2, \cdots, \theta_6) \quad (16)$$

The applied kriging formulation is independent of σ_Y^2. Thus the parameter is not identifiable and is not included in the set of model parameters in (16).

The fourth inverse model, F4, deals with zonation of the Y field, where the mean log transmissivities in each zone are the unknown parameters to be optimized. In the literature, the zonation approach is used frequently [e.g., *Emsellem and de Marsily*, 1971; *Cooley*, 1977]. In the present study the number of model parameters is harmonized by dividing the aquifer into seven zones

$$\mathbf{p}_{f_4} = (Y_{z_1}, Y_{z_2}, \cdots, Y_{z_7}) \quad (17)$$

Neuman and Yakowitz [1979] incorporate prior information into the zonation approach by adding a penalty term to the objective function. The penalty term is a functional of the departures of the estimated zonal transmissivities from prior values. By constraining the estimates the stability of the solution is increased.

However, to simplify a comparison between the four approaches the parameter identification procedure (including the minimizing criterion) is kept identical, so the addition of a penalty term to the objective function of the F4 model is not included in this study.

2.4. *Parameterization and Initial Parameter Estimates*

Before starting up the inverse models, determination of the pilot point locations of F1 and the zonation patterns of F2 and F4, respectively, is required. This task is performed by trial and error minimization of the fit criterion (5). For the F1 model, the best results have been obtained by concentrating the pilot points in limited domains of the aquifer. To begin with, the most sensitive regions were identified by distributing the pilot points evenly throughout the aquifer. For the F2 and the F4 models, the starting point of the zonation pattern adjustments is based on plots of the initially kriged distributions of the transmissivity. In most cases, the final zonation pattern has been close to the isoline structure of the kriged field.

Finally, initial values of the unknown model parameters must be specified for the optimization algorithm. To make the procedure as objective as possible, the initial estimates of $\mathbf{p}_f$ are calculated based on the discrete observations of the transmissivity, as described below.

For the F1 model, the unknown log transmissivities at the pilot points are initialized by point kriging, based on the N observed values. The same initial transmissivity distribution is used in the F2 model by setting the correcting factors in (13) to zero.

For the F3 model, the trend of the Y field is initially expressed by the best linear regression model based on the Y observations only. With respect to the reciprocal correlation length α, the autocovariance function (15) implies

$$\alpha = \frac{1}{r}\left[-\ln \frac{\mathrm{Cov}_Y(r)}{\sigma_Y^2}\right]^{1/2} \quad (18)$$

Given N Y data, $N(N-1)/2$ pairs of different observations $(\bar{Y}_i, \bar{Y}_j)$ can be selected. As a first guess, α is set equal to the mean of the $N(N-1)/2$ terms

$$\frac{1}{r}\left\{-\ln\left[\frac{(\bar{Y}_i - \bar{Y}_i)(\bar{Y}_j - \bar{Y}_j)}{\frac{1}{2}[(\bar{Y}_i - \bar{Y}_i)^2 + (\bar{Y}_j - \bar{Y}_j)^2]}\right]\right\}^{1/2} \quad (19)$$

In (19) an overbar designates the initial regression-estimated trend values at the actual data points, while r denotes the spatial distance between the data points.

The unknown zonal log transmissivities of the F4 model are initially calculated using the kriging model of F1 and F2. This was accomplished by modifying the kriging formulation to work with region-integrated semivariogram values.

3. TEST PROGRAM

3.1. *The Synthetic Transport Problem*

The inverse models are applied to a synthetic two-dimensional problem. Figure 2 shows the finite difference discretization, the boundary conditions, and the location of the solute source of the hypothetical aquifer. The synthesized source concentration is 1000 mg/L. The log transmissivities are generated as a Gaussian-distributed stochastic process using the turning bands method [*Mantoglou and Wilson*, 1982], in which an exponential autocovariance function is used to incorporate spatial correlation. The generated field is isotropic, and the correlation length is 400 m. A linear trend of 0.5/km is added to the generated stationary field. The "real" stationary head distribution and the "real" nonstationary solute spreading are calculated by using the final transmissivity field as input to the MOC model. From the constructed transport problem, 20 head values and five simultaneous concentration values (18-year transport period) are selected as "observation" data. Figure 2 shows the locations of the "observations" in the quadratic aquifer with side length 4000 m.

The inverse approaches are applied to four test cases which differ in the variability of the generated log transmissivity field and with respect to the amount and accuracy of the "observed" transmissivities. Test case 1 is used as a reference case. In test cases 1 and 2 the log transmissivities are generated with different values of the Gaussian variance to compare the ability of the models to reproduce fields of different complexity. Test cases 1 and 3 use different numbers of Y "observations" to compare the sensitivity of the models to the amount of prior information. Test cases 1 and 4 use exact and noisy Y "observations," respectively, to compare the sensitivity of the models to the quality of the prior information. The pilot point locations of F1 and the zonation patterns of F2 and F4 are adjusted in each of the test cases 1–3 to obtain the best overall fit of the flow and

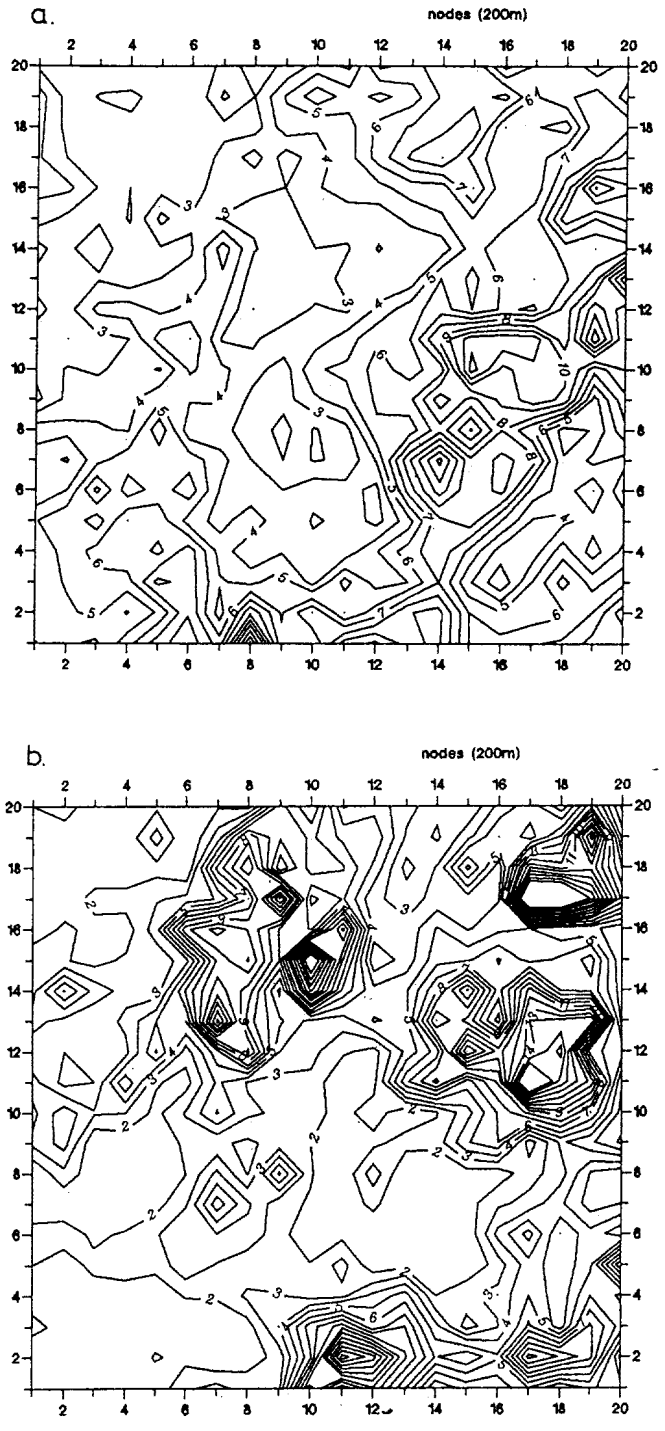

Fig. 4. The two generated transmissivity fields: (*a*) test case 1; (*b*) test case 2 (transmissivities are in 1000 m^2/s).

predicted solute transport. In model F3, even a second-order trend in the transmissivity field seems inadequate when dealing with the complex transmissivity field of test case 2.

3.6. . *Test Case 3*

In the third test case the number of transmissivity observations is reduced from 10 to five. The selected locations appear in Figure 2. The transmissivity field of case 1, which was generated with a variance of 0.4, is applied. Table 5 and Figure 7 show the simulation results.

The deteriorations of the test measures of F3 are the most significant, which emphasizes the strong dependence of F3 on the T data. F1 and F2 perform relatively better with respect to compensation for the reduced information. While the fewer T observations reduce the basis for the kriging approaches, F4 is unaffected by the altered conditions and becomes now superior.

As regards model fit, the F1 model generates better measures than the F2 model at the time of observation, while the future predictions indicate F2 to be the most reliable of the two approaches. This phenomenon is due to the difference between the "point correction" approach of F1 and the "zonal correction" approach of F2. The ability of F1 to affect the kriged structure at the local scale makes it flexible enough to fit the observed "short-time" migration of the plume, but the continued simulation of the plume is more exposed to distortion when based on these large local-scale corrections than the regional-scale corrections implied by F2.

3.7. *Test Case 4*

While the selected transmissivity observations of the first three test cases are the exact generated values, the effect of noisy transmissivity data is examined in the fourth test case. Ten vectors of independent Gaussian noise are generated with zero mean and a variance of 0.4. The noise vectors are added to the "observed" log transmissivities of case 1, thereby constructing 10 sets of noisy data.

The averaged test measures from the application of the inverse models F1, F2 and F3 to the noisy data are shown in Table 6. The change in the measures from the results of case 1 also is shown. The F4 model is not included because of the independence of the T data.

The simulation accuracy of all three models was reduced considerably by the added noise. F1 and F3 are apparently most sensitive to measurement errors, while F2 better compensates for the noisy T data. In this case the F2 model benefits from the zonation part of the "mixed" approach by which it acquires the ability to moderate the regional influence of an erroneous kriging observation.

TABLE 3. Simulation Results of Test Case 1

Model	HDF, m^2	HMF, m^2	CDF_{18}	CMF_{18}	CMF_{40}	CPU Time, min
F1	0.0040	0.0031	0.0019	0.0045	0.0038	165
F2	0.0039	0.0031	0.0029	0.0026	0.0043	110
F3	0.0070	0.0075	0.0039	0.0034	0.0017	75
F4	0.0047	0.0032	0.0003	0.0018	0.0018	183

TABLE 2. Results of Semivariogram Parameter Optimizations

Model	$\hat{\omega}$	$\hat{a}$, m	$\hat{\lambda}$	Min (NLL)
		Test Case 1		
exponential	0.256	901.	···	12.
gaussian	0.326	1086.	···	10.
monomial	0.184	···	0.414	13.
		Test Case 2		
exponential	1.0*	3040.	···	17.
gaussian	0.440	1070.	···	13.
monomial	0.304	···	1.0*	17.

Three log transmissivity semivariogram formulations are applied to two data sets of test case 1 and test case 2, respectively.
*Upper bound of parameter range.

information about the Y field except the Y observations is assumed available. Therefore, the applied stationarity-based procedures will to some extent fail in selecting the "true" semivariogram. Three different semivariogram formulations are optimized according to the methodology described in section 2.3. The tested formulations are the exponential,

$$\gamma(r) = \omega\left[1 - \exp\left(-\frac{r}{a}\right)\right] \tag{25}$$

the Gaussian,

$$\gamma(r) = \omega\left[1 - \exp\left(-\frac{r^2}{a^2}\right)\right] \tag{26}$$

and the monomial,

$$\gamma(r) = \omega r^{\lambda} \tag{27}$$

In (25)–(27), γ is the semivariogram, and r is the spatial lag. The results of the parameter optimizations are listed in Table 2. In both cases the Gaussian formulation is selected, as this model leads to the smallest minimum value of the NLL. In Figure 3 the optimized models are compared with the corresponding sampled semivariograms.

3.4. *Test Case 1*

In the first test case, a log transmissivity field with a variance of 0.4 is generated (see Figure 4*a*). The locations of the 10 transmissivities selected as "observations" are shown in Figure 2. Test case 1 acts as a reference case. The simulation results are listed in Table 3 as measures of data and model fit. The model fit measures (22)–(24) are visualized for each of the four approaches in Figure 5. The large plots show the accuracy of the future predictions (CMF_{40}), and the small plots in the corners are the fit at the time of observation (CMF_{18}). The fit of the stationary head distributions also is shown in the small plots (HMF). "Observed" head and concentration are contoured from the full grid values produced by the "true" simulations.

The results document the suitability of the reference case: Except for some poor head measures of F3 no significant differences are revealed among the test measures of the four approaches. The ability of F3 to fit the head data varies over the aquifer, while the simulation accuracy of the other approaches is more homogeneous. In fact, the F3 model reproduces the aquifer very well downstream of the source, which implies a close fit of the predicted plume. On the other hand, the optimized trend causes extreme transmissivity

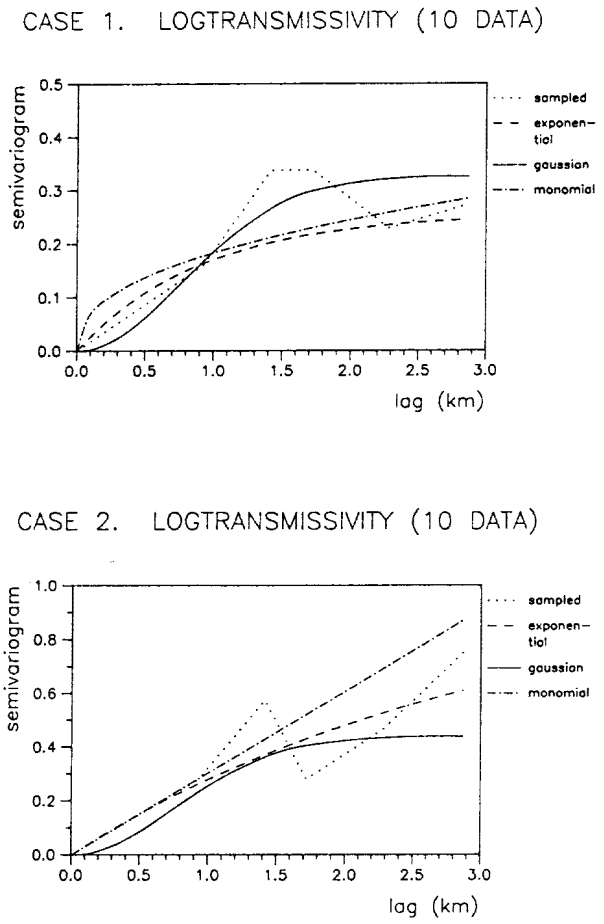

Fig. 3. Sampled and optimized log transmissivity semivariograms: (*a*) test case 1; (*b*) test case 2. In both cases the semivariograms are based on 10 selected point "observations."

estimates upstream of the source, and the incorporated transmissivity observations are inadequate to influence the kriging estimates in this region.

3.5. *Test Case 2*

In the second test case the variability of the log transmissivities is increased. The distribution is generated as in case 1, but the variance equals 0.7. The numbers and locations of the observation data are unchanged. Figure 4*b* shows the generated field of test case 2. Table 4 lists the values of the test measures, and Figure 6 shows the corresponding model fits.

When applied to this more complex T field, the results of F3 and F4 are inferior to the results of F1 and F2. The ability of the F1 model to reproduce large local heterogeneities is due to the possibility of clustering the pilot points in regions of particular complexity. The F4 model fails somewhat because its ability to identify variabilities beyond the regional scale is too limited. If prior transmissivity information is taken into account by adding a penalty term to the objective function as described in section 2.3, the future simulation might be improved due to more plausible estimates. Here we have found, however, that the combined zonation and kriging approach of F2 is superior to F4 as regards both the fit of the head field and the reliability of the

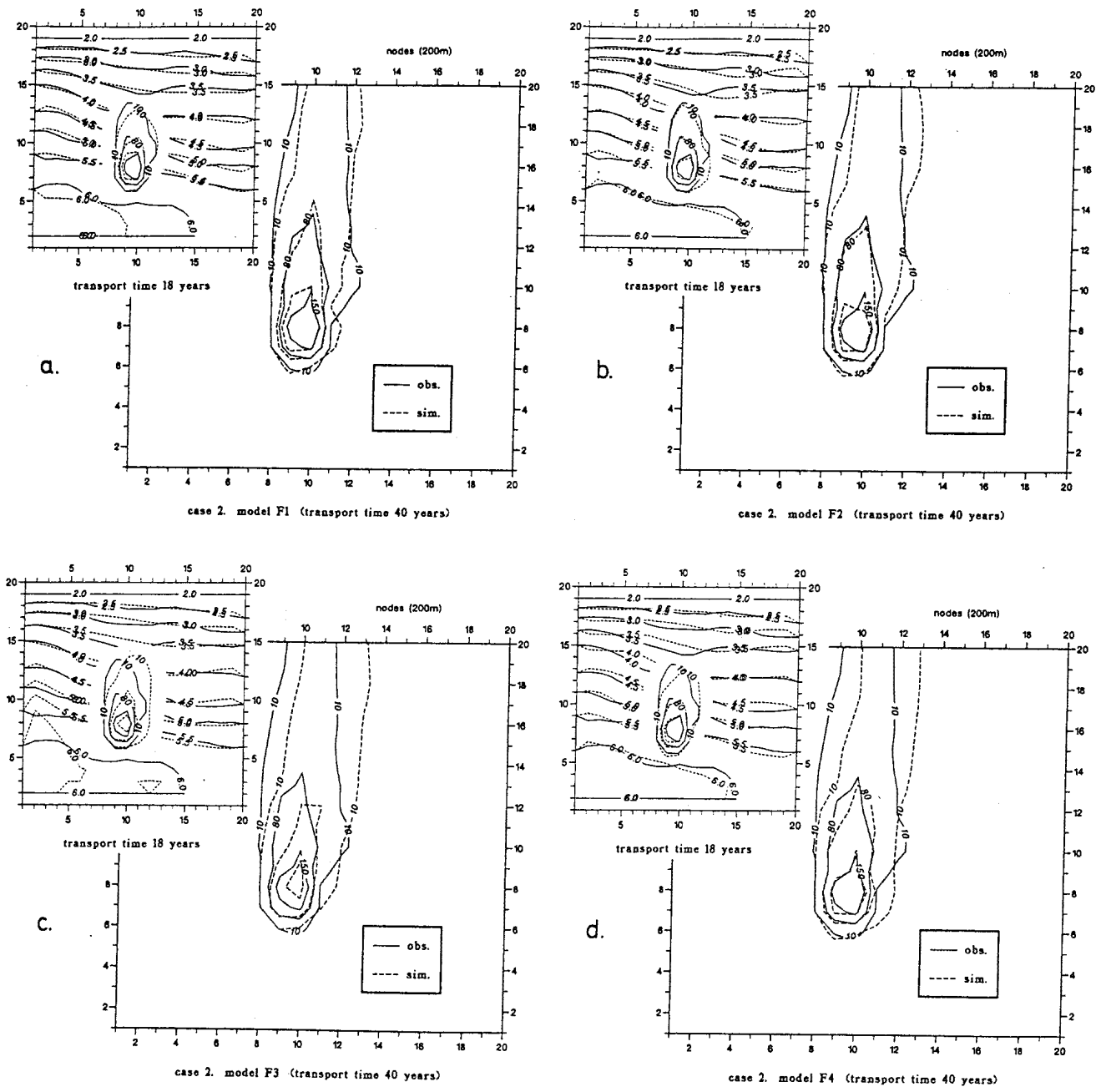

Fig. 6. Same as Figure 5, but for test case 2.

selected. Case 4.1 designates the application of F1 and F2 to this specific data set using the pilot point locations and zonation pattern from case 1. In case 4.2 the pilot points and the zonation are adjusted according to the new conditions caused by the added noise. In case 4.3 the geostatistical model obtained by the semivariogram analysis is replaced by that optimized by F3. The simulation results are listed in Table 7, and Figures 8, 9, and 10 compare the obtained model fits of the three cases 4.1, 4.2 and 4.3.

For both F1 and F2, the simulation is improved consider-

TABLE 5. Simulation Results of Test Case 3

Model	HDF, m^2	HMF, m^2	CDF_{18}	CMF_{18}	CMF_{40}	CPU Time, min
F1	0.0040	0.0028	0.0035	0.0032	0.0064	64
F2	0.0032	0.0039	0.0005	0.0108	0.0061	255
F3	0.0092	0.0065	0.0092	0.0230	0.0088	145
F4	0.0047	0.0033	0.0005	0.0018	0.0029	72

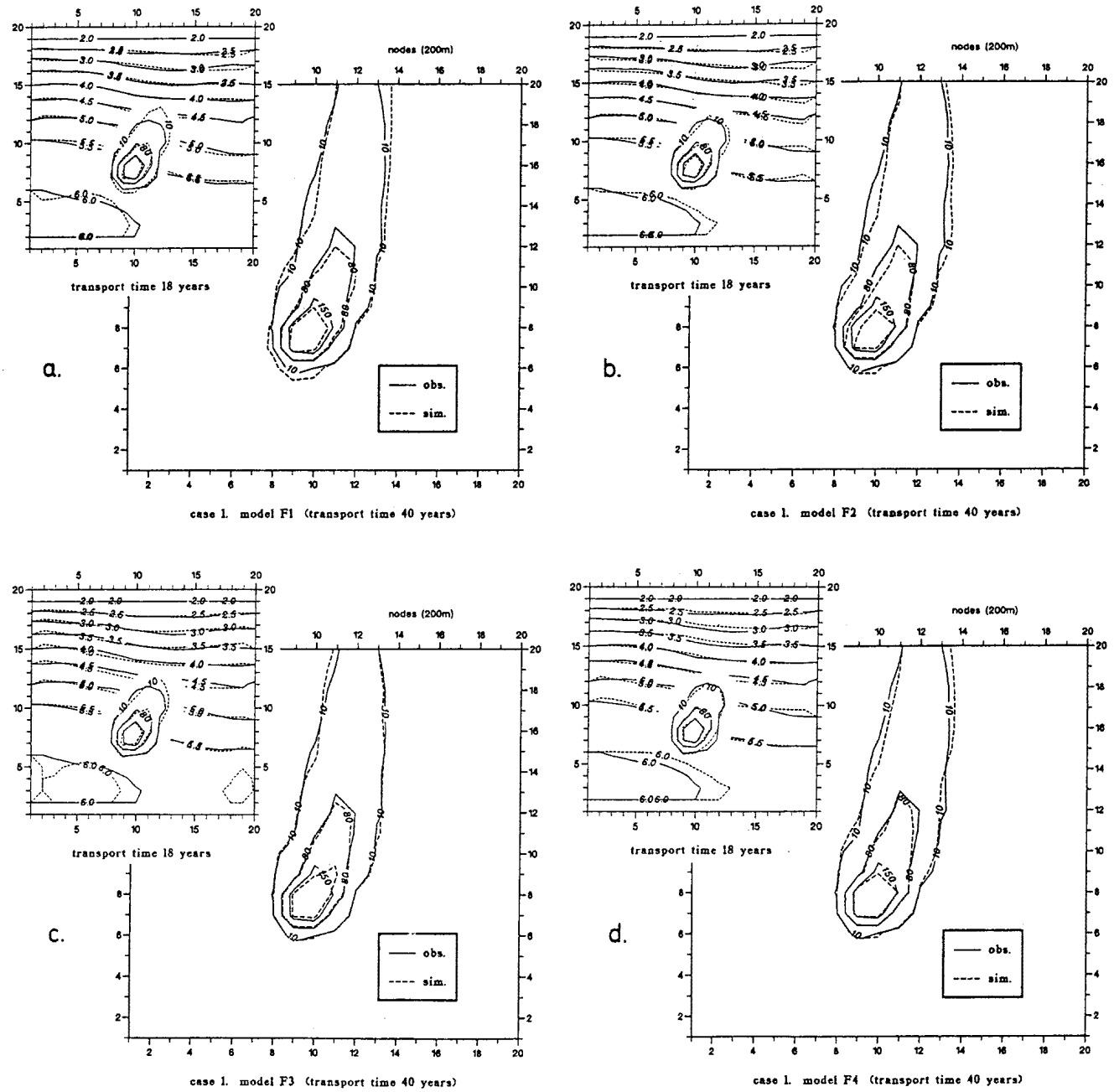

Fig. 5. Model fits by application of the four optimization models to test case 1: (*a*) model F1; (*b*) model F2; (*c*) model F3; (*d*) model F4. The large plumes are future simulations, and the small plots are at the time of observation (head is in meters and concentration is in milligrams per liter).

In the application of models F1 and F2 to the 10 sets of the noisy T data, the pilot point locations and zonation pattern were kept unchanged from the optimum distributions obtained with the exact data in case 1. To evaluate the sensitivity of F1 and F2 to the locations of pilot points and regions, respectively, and to the identified geostatistical model, additional tests were carried out. For that purpose the noisy data set that led to the poorest test measures was

TABLE 4. Simulation Results of Test Case 2

Model	HDF, m^2	HMF, m^2	CDF_{18}	CMF_{18}	CMF_{40}	CPU Time, min
F1	0.0041	0.0058	0.0033	0.0056	0.0108	117
F2	0.0045	0.0068	0.0025	0.0061	0.0101	160
F3	0.0096	0.0131	0.0264	0.0292	0.0346	144
F4	0.0087	0.0092	0.0023	0.0061	0.0318	153

TABLE 7. Simulation Results of Test Case 4.1, 4.2, and 4.3

Case	HDF, m^2	HMF, m^2	CDF_{18}	CMF_{18}	CMF_{40}	CPU Time, min
			Model F1			
4.1	0.0210	0.0329	0.0243	0.0345	0.0556	213
4.2	0.0124	0.0272	0.0098	0.0257	0.0464	224
4.3	0.0032	0.0184	0.0074	0.0246	0.0156	489
			Model F2			
4.1	0.0144	0.0203	0.0052	0.0313	0.0248	517
4.2	0.0039	0.0112	0.0061	0.0174	0.0094	328
4.3	0.0047	0.0121	0.0061	0.0081	0.0082	257

ably from case 4.1 to case 4.2, thereby revealing the models to be very sensitive to pilot point locations and zonation pattern, respectively. Still, F1 is inferior to F2 with respect to its ability to compensate for the noisy data. When using the geostatistics optimized by F3, the improvements of the F1-based simulations are pronounced, which shows the approach to be very sensitive to the applied geostatistical model. The overall fit of the head is improved, which implies that the future prediction of the plume is more reliable. As regards F2, no significant improvement is obtained. This limited sensitivity to the geostatistical model indicates that the approach is relatively robust to model errors (i.e., errors caused by model approximations in contrast to measurement errors).

3.8. *Comments on the Optimization Process*

For each of the four tested inverse approaches the consumption of CPU time differs from one optimization problem to another. However, considering many optimizations, no one of the formulations is clearly more efficient. This is illustrated by the computational costs of the 10 optimizations of case 4. When comparing the three involved models, the averaged costs of the computer runs are almost equal (see Table 6). But, if the time consumed during the initial trial and error optimization of pilot point locations or zonation pattern is included, then F3 is most efficient. As regards the initial determination of the pilot point locations of F1 and zonation patterns of F2 and F4, respectively, four to eight adjustments were required.

4. SUMMARY AND CONCLUSIONS

Four inverse approaches in two-dimensional groundwater transport modeling have been compared. The approaches differ in the way spatially variable transmissivities are modeled. However, the number of model parameters and thus the degrees of freedom are the same in each approach. The approaches are based on the two-stage feedback method, and the focus has been on the estimation of transmissivity. Four test cases which differ in the variability of the transmissivity field and with respect to the quantity and quality of the input transmissivity data were constructed.

The first approach, F1, estimates log transmissivities at selected "pilot points" which, with measured values at observation points, are used to produce a transmissivity distribution by kriging. In spite of its apparent flexibility, this approach did not perform well in the presence of measure-

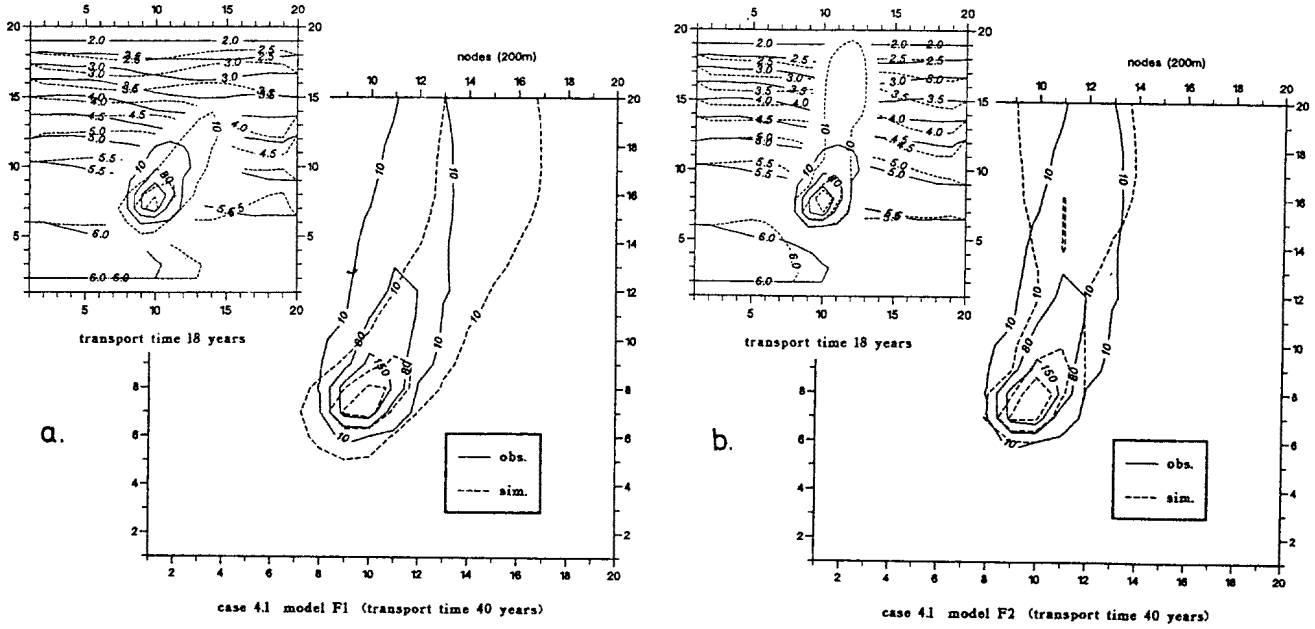

Fig. 8. Model fits by application of two selected optimization models to test case 4.1: (*a*) model F1; (*b*) model F2. (Head is in meters and concentration is in milligrams per liter.)

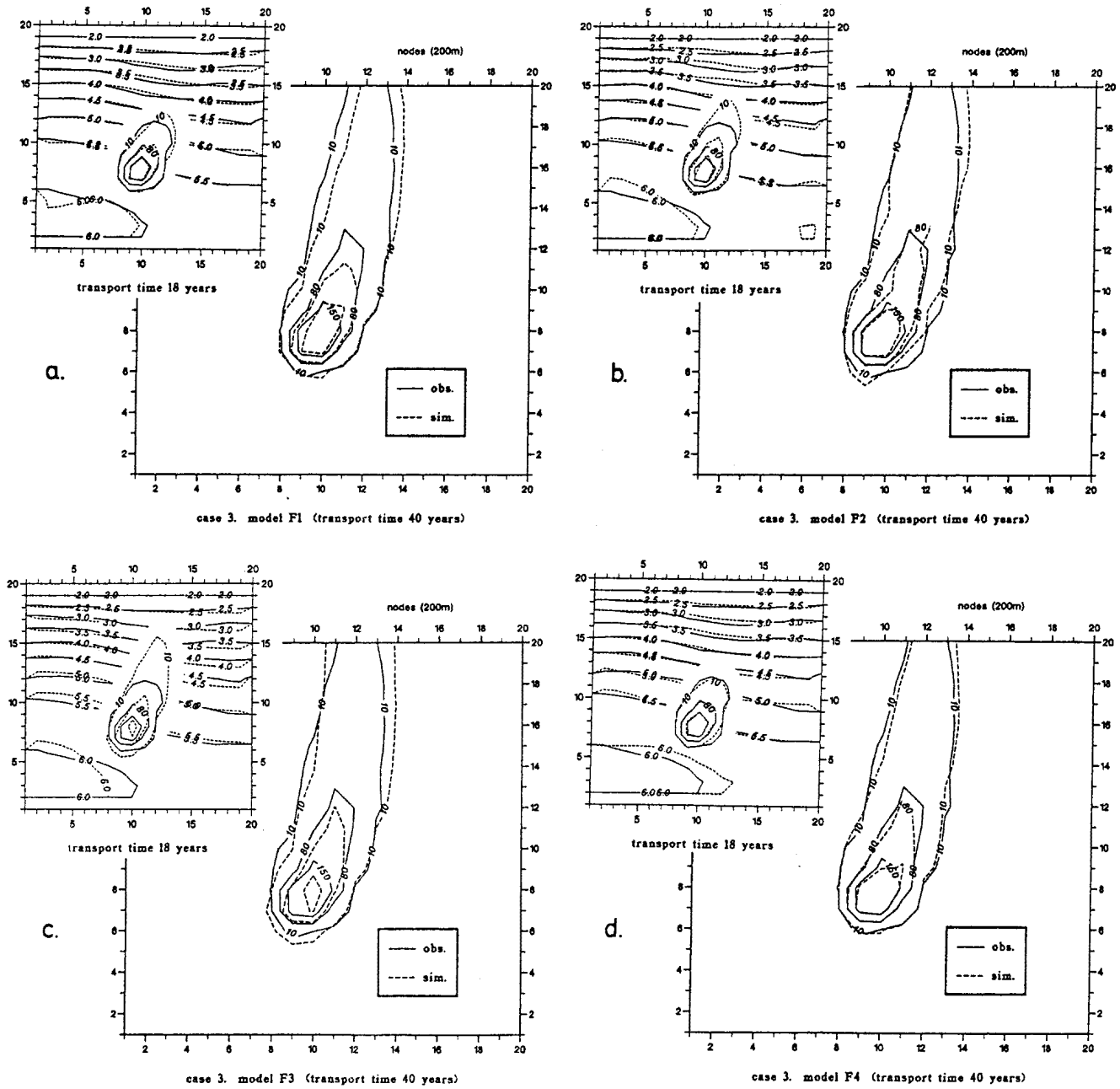

Fig. 7. Same as Figure 5, but for test case 3.

TABLE 6. Simulation Results of Test Case 4

Model	HDF (ΔHDF), m^2	HMF (ΔHMF), m^2	CDF_{18} (ΔCDF_{18})	CMF_{18} (ΔCMF_{18})	CMF_{40} (ΔCMF_{40})	Averaged CPU Time, min
F1	0.0088	0.0112	0.0085	0.0175	0.0181	243
	(+0.0047)	(+0.0081)	(+0.0066)	(+0.0130)	(+0.0143)	
F2	0.0071	0.0084	0.0053	0.0145	0.0094	268
	(+0.0031)	(+0.0053)	(+0.0024)	(+0.0119)	(+0.0051)	
F3	0.0138	0.0155	0.0105	0.0205	0.0122	280
	(+0.0068)	(+0.0080)	(+0.0066)	(+0.0171)	(+0.0105)	

The listed test measures are averaged values from the 10 model runs with noisy T data. The differences from the measures of test case 1 (exact T data) are also given.

other hand, the model is quick and easy to use because no prior geostatistical analysis or determination of the physical model (e.g., zonation pattern) have to be carried out. The approach could be used to optimize the geostatistics as input to the first two approaches, which also are based on kriging.

The fourth approach, F4, is the pure zonation approach. The aquifer is divided into subregions of homogeneous transmissivities, which are optimized by the model. The approach does not incorporate T observations. In spite of the simplicity of the approach it is generally superior to the data-dependent approaches in cases of limited data availability and poor data quality. However, when applied to fairly complex aquifers it does fail somewhat. In this case, the prediction performance will possibly be improved by incorporating the transmissivity information more directly in an extended objective function, comprising a term that penalizes departures from prior estimates.

REFERENCES

Adar, E. M., S. P. Neuman, and D. A. Woolhiser, Estimation of spatial recharge distribution using environmental isotopes and hydrochemical data, I, Mathematical model and application to synthetic data, *J. Hydrol.*, *97*, 251–277, 1988.

Bear, J., *Dynamics of Fluids in Porous Media*, American Elsevier, New York, 1972.

Carrera, J., State of the art of the inverse problem applied to the flow and solute equations, Groundwater Flow and Quality Modelling, *NATO ASI Ser., Ser. C*, *224*, 549–584, 1987.

Cooley, R. L., A method of estimating parameters and assessing reliability for models of steady state groundwater flow, *Water Resour. Res.*, *13*(2), 318–324, 1977.

Dagan, G., Stochastic modeling of groundwater flow by unconditional and conditional probabilities, 2, The solute transport, *Water Resour. Res.*, *18*(4), 835–848, 1982.

de Marsily, G., et al., Interpretation of interference tests in a well field using geostatistical techniques to fit the permeability distribution in a reservoir model, in *Geostatistics for National Resources Characterization*, edited by G. Verly, M. David, A. G. Journel, and A. Marechal, pp. 831–849, D. Reidel, Hingham, Mass., 1984.

Emsellem, Y., and G. de Marsily, An automatic solution for the inverse problem, *Water Resour. Res.*, *7*(5), 1264–1283, 1971.

Freeze, R. A., A stochastic-conceptual analysis of one-dimensional groundwater flow in a nonuniform homogeneous medium, *Water Resour. Res.*, *11*(5), 725–741, 1975.

Gorelick, S. M., B. Evans, and I. Remson, Identifying sources of groundwater pollution: An optimization approach, *Water Resour. Res.*, *19*(3), 779–790, 1983.

Hoeksema, R. J., and P. K. Kitanidis, An application of the statistical approach to the inverse problem in two-dimensional groundwater modeling, *Water Resour. Res.*, *20*(7), 1003–1020, 1984.

IMSL FORTRAN subroutines for mathematical applications, users manual, version 1.0, vol. 3, pp. 847–852, 876–881, Houston, Tex., 1987.

Keidser, A., D. Rosbjerg, K. Høgh Jensen, and K. Bitsch, A joint kriging and zonation approach to inverse groundwater modelling, Calibration and Reliability in Groundwater Modelling, *IAHS Publ. 195*, 171–184, 1990.

Kitanidis, P. K., and E. G. Vomvoris, A geostatistical approach to the inverse problem in groundwater modeling (steady state) and one-dimensional simulations, *Water Resour. Res.*, *19*(3), 677–690, 1983.

Knopman, D. S., and C. I. Voss, Discrimination among one-dimensional models of solute transport in porous media: Implications for sampling design, *Water Resour. Res.*, *24*(11), 1859–1876, 1988.

Konikow, L. F., and J. D. Bredehoeft, Computer model of two-dimensional solute transport and dispersion in groundwater, book 7, chap. C2, U.S. Geol. Surv., Reston, Va., 1978.

Kuiper, L. K., A comparison of several methods for the solution of the inverse problem in two-dimensional steady state groundwater flow modeling, *Water Resour. Res.*, *22*(5), 705–714, 1986.

Mantoglou, A., and J. L. Wilson, The turning bands method for simulation of random fields using line generation by a spectral method, *Water Resour. Res.*, *18*(5), 1379–1394, 1982.

Murphy, V. V. N., and V. H. Scott, Determination of transport model parameters in groundwater aquifers, *Water Resour. Res.*, *13*(6), 941–947, 1977.

Neuman, S. P., and S. Yakowitz, A statistical approach to the inverse problem of aquifer hydrology, 1, Theory, *Water Resour. Res.*, *15*(4), 845–860, 1979.

Samper, F. J., and S. P. Neuman, Estimation of spatial covariance structures by adjoint state maximum likelihood cross validation, 1, Theory, *Water Resour. Res.*, *25*(3), 351–362, 1989.

Strecker, E. W., and W. Chu, Parameter identification of a groundwater contaminant transport model, *Ground Water*, *24*(1), 56–62, 1986.

Umari, A., R. Willis, and P. L.-F. Liu, Identification of aquifer dispersivities in two-dimensional transient groundwater contaminant transport: An optimization approach, *Water Resour. Res.*, *15*(4), 815–831, 1979.

Van Rooy, D., A. Keidser, and D. Rosbjerg, Inverse modelling of flow and transport, Groundwater Contamination, *IAHS Publ.*, *185*, 11–23, 1989.

Wagner, B. J., and S. M. Gorelick, Optimal groundwater management under parameter uncertainty, *Water Resour. Res.*, *23*(7), 1162–1174, 1987.

Yeh, W. W.-G., Review of parameter identification procedures in groundwater hydrology: The inverse problem, *Water Resour. Res.*, *22*(2), 95–108, 1986.

A. Keidser and D. Rosbjerg, Groundwater Research Centre, Building 115, Technical University of Denmark, DK-2800 Lyngby, Denmark.

(Received May 30, 1990;
revised March 26, 1991;
accepted April 3, 1991.)

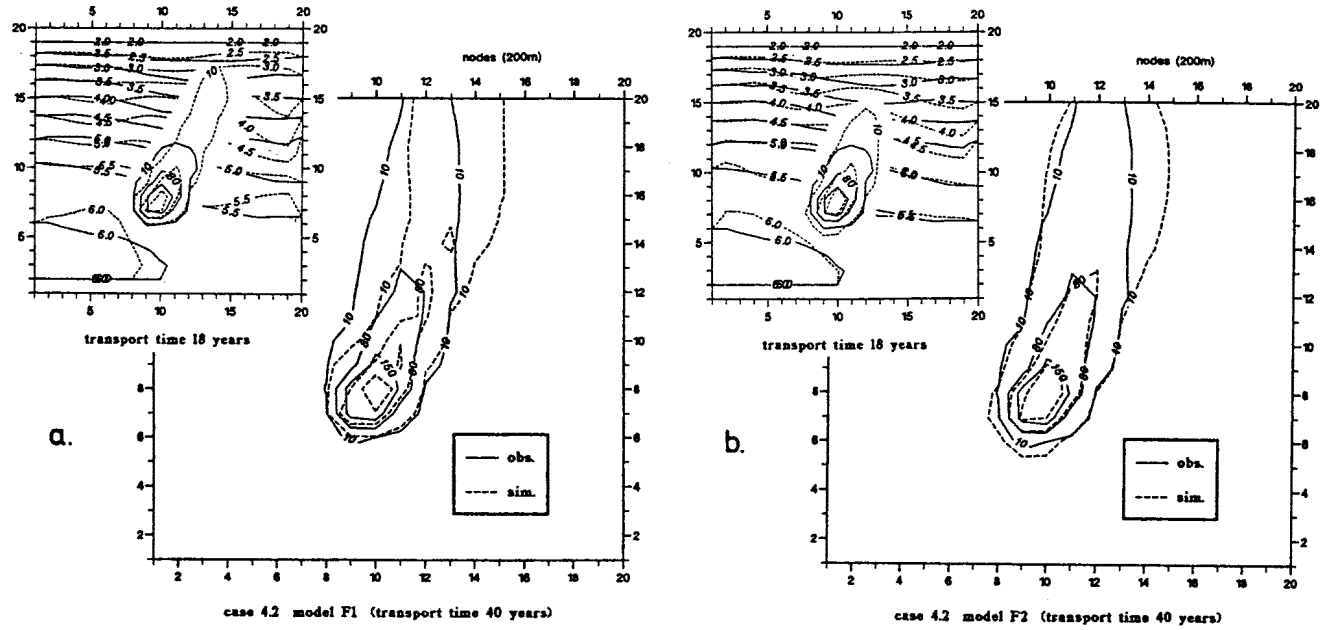

Fig. 9. Same as Figure 8, but for test case 4.2.

ment and model errors. However, the approach is the best at reproducing large local heterogeneities due to the influence of the pilot points on the kriged T field.

The second approach, F2, uses kriging, too, but "correcting terms" proportional to the kriging standard deviations are added to the kriging estimates. The proportional factors, which apply to specific regions, are optimized. This joint kriging and zonation approach seems to be suitable to all-round applications: Because of the flexibility of the zonation it generally performs better than the two other kriging approaches. Additionally, the model seems to be robust to erroneous geostatistical formulations. Compared to the pure zonation approach it profits by the incorporated transmissivity information when applied to aquifers of increasing variability. On the other hand, it becomes inferior to the pure zonation approach in the case of data scarcity or measurement errors.

The third approach, F3, estimates the trend and the correlation length of the log transmissivity, and the entire distribution is estimated by kriging. Contrary to the two other kriging approaches, prior knowledge of the covariance structure is not implied in this case. This approach is very sensitive to the number and the reliability of T data, and simulation accuracy is strongly dependent on how closely the T data represent the true distribution. Further, the approach is inferior when applied to complex T fields. On the

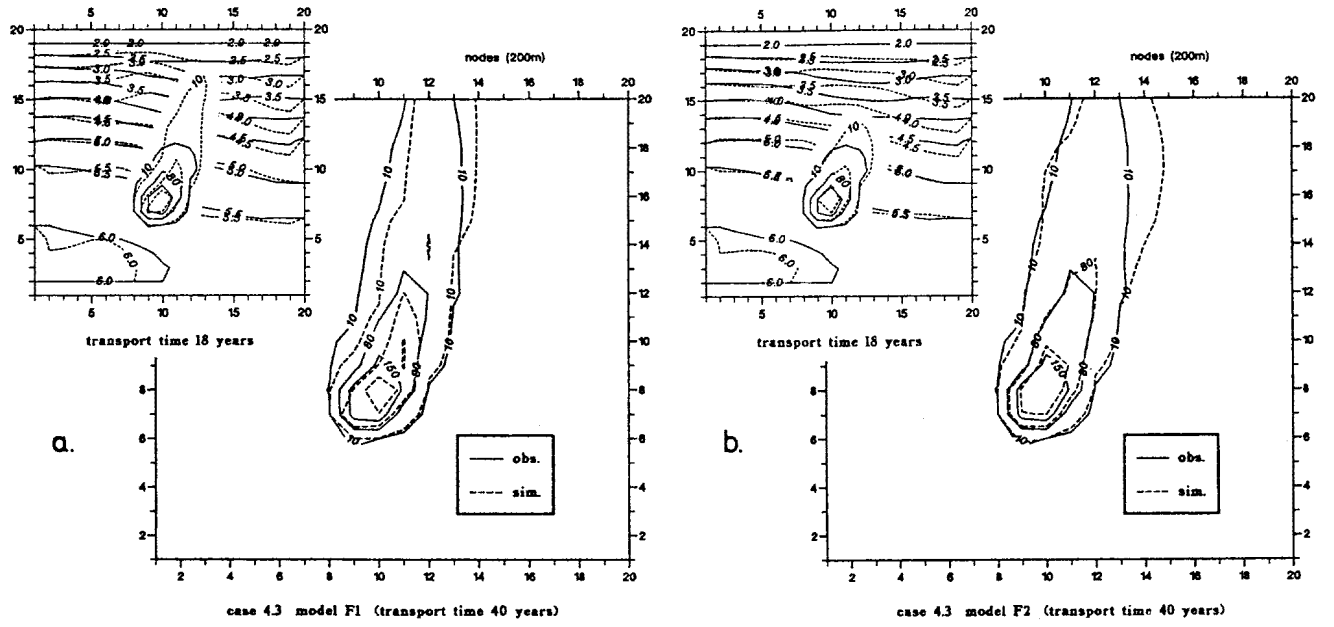

Fig. 10. Same as Figure 8, but for test case 4.3.